
Speeding-up One-vs-All Training for Extreme Classification via Smart Initialization

Erik Schultheis

Department of Computer Science
Aalto University
Helsinki, Finland
first.last@aalto.fi

Rohit Babbar

Department of Computer Science
Aalto University
Helsinki, Finland
first.last@aalto.fi

Abstract

In this paper we show that a simple, data dependent way of setting the initial vector can be used to substantially speed up the training of linear one-versus-all (OVA) classifiers in extreme multi-label classification (XMC). We discuss the problem of choosing the initial weights from the perspective of three goals. We want to start in a region of weight space a) with low loss value, b) that is favourable for second-order optimization, and c) where the conjugate-gradient (CG) calculations can be performed quickly. For margin losses, such an initialization is achieved by selecting the initial vector such that it separates the mean of all positive (relevant for a label) instances from the mean of all negatives – two quantities that can be calculated quickly for the highly imbalanced binary problems occurring in XMC. We demonstrate a speedup of $\approx 3\times$ for training with squared hinge loss on a variety of XMC datasets. This comes in part from the reduced number of iterations that need to be performed due to starting closer to the solution, and in part from an implicit negative mining effect that allows to ignore easy negatives in the CG step. Because of the convex nature of the optimization problem, the speedup is achieved without any degradation in classification accuracy.

1 Introduction

Extreme Classification In this work we consider *extreme multi-label classification* (XMC) problems. Here, the number of labels l is very large (possibly in the millions). Such problems arise in various domains such as annotating large encyclopedia [28], image-classification [9], next word prediction [26, 27], as well as recommendation systems, web-advertising and prediction of related searches [2, 29, 17].

We assume that the fraction of positive training instances for most labels is very low – the label frequency has a long-tailed distribution [8]. This is a good approximation e.g. for the large dataset from the extreme classification repository [5] (cf. Figures 1 in [31, 4, 28] for some examples), and for many types of data that is gathered at internet-scale [1].

One-vs-All Classifiers Many XMC methods employ some form of a *one-vs-all* (OvA) classifier as the last stage of the classification procedure, in the sense that for a data point \mathbf{x} with corresponding features $f(\mathbf{x})$ and label $y \in \{-1, 1\}$, the predictions are calculated as

$$\text{top}_k\{\mathbf{w}_i^\top f(\mathbf{x}) : i \in [l]\} \quad (1)$$

and the training objective is to minimize (with some additional regularization terms)

$$\phi(y_i \mathbf{w}_i^\top f(\mathbf{x}_i)), \quad (2)$$

where ϕ denotes some margin loss and y_i is the corresponding label. Algorithms that follow this general structure are DiSMEC [4] and ProXML [3] for sparse representations f , and Slice [17] where f is some pre-trained mapping of instances to dense vectors. Other examples are Parabel [30] and PPDsparse [36]. Embedding-based approaches where the mapping f itself is learnt, such as XML-CNN [19, 37] are incompatible with the method presented in this paper. However, in some cases, even though f is not parameter-free, it is only fine-tuned during the OvA training, as is the case in Astec [7].

Fast Training Minimizing this objective using a gradient-based iterative algorithm is very computation-intensive. To reduce compute requirements – and thus energy consumption – we can make use of three generic principles

1. Try to achieve more progress per step, e.g. by using a second-order method [4, 18, 13] or an adaptive step size. [10, 33]
2. Make the computations of each step faster, e.g. by approximating the true loss with negative mining [17, 7, 30, 36, 32].
3. Reducing the number of necessary steps by taking a good initial guess for the weight vector. [12, 18]

In this work, we focus on the second-order optimization approach using a truncated conjugate-gradient (CG) Newton optimization, as it is used in recent versions of Liblinear [13] (older versions [11] were using a trust-region Newton method).

Implicit Negative-Mining with Hinge-Like Losses To a certain degree, the second point is achieved implicitly when using a loss function that becomes zero once the point is classified correctly with sufficient margin. In that case, such a training point makes no contribution to the gradient or Hessian, and thus can be skipped in these computations. This can be seen as an implicit negative mining, where the list of negatives is updated each iteration (similar to Yen et al. [36]) based on the values of $y_i \mathbf{w}_i^\top f(\mathbf{x}_i)$. Unlike explicit negative mining, this is not an approximation, but it also does not enforce sparsity but only exploits it when it exists. Fortunately, close to convergence when most instances are correctly classified, this leads to very sparse computations for the CG procedure. Thus one of our goals is to get into this fast regime as quickly as possible.

Choice of Initial Vector The third idea is used in Liblinear to speed up hyperparameter sweeps. It is assumed that the solutions for two similar hyperparameter values are closely related, and as such the final weight vector of one training run can be used to warm start the next. The feasibility of this approach in (cold-start) XMC has been shown in Fang et al. [12]. The basic motivation is given by

their Lemma 3.1, which states that if two label vectors are similar (measured in Hamming distance), then the optimal weight vectors with respect to a Lipschitz loss are also similar.

The strategy is thus to train the optimal weight vector for a virtual label that has only negatives. Such a label vector has small Hamming distance to all the label vectors of tail labels, and thus provides a good candidate for a starting vector. They call this strategy *OvA-Primal* (OvAP).

They extend this idea by building a *minimum spanning tree* (MST) over the labels (plus the virtual all-negative label at the root), and then training in such an order that during each training process the trained weights of a label that is very similar to the target label can be reused. This is called OvAP++.

Shortcomings of the Existing Work OvAP is very simple and easy to implement, but it completely ignores the positive labels for each instance. We will show that there is a computationally cheap method that allows taking them into account.

In contrast, OvAP++ makes use of the positives, but requires much more care to implement, as it breaks the embarrassingly parallel nature of the original OvA approach. Now the individual binary problems need to be solved in a certain (partial) order. This also precludes the application of this strategy to situations where all labels have to be trained simultaneously, e.g. when fine-tuning the feature representations f .

The evaluation of that strategy has not been done on datasets which are very large and show extreme tail-label behaviour (Wiki31K is the most "extreme" dataset they have used). In such a situation, the speed-up due to the tree procedure might not be very large, because the tail-labels will not have overlapping positives. This is supported by [12, Lemma 3.2], which implies that two labels with non-overlapping positives need not be considered for the MST. Since the root node is fixed by construction to be the all-zero label, this is likely to lead to a graph for which most of the nodes (corresponding to the tail labels) are direct children of the root, and are trained exactly as they would without the MST.

Important properties of the loss function (such as local smoothness / Lipschitz constant) sometimes are more favourable after some training epochs than right at initialization time, as evidenced e.g. by the success of cyclical learning rates [34] and warmup phases [15]. However, the existing analysis focuses only on finding an initial weight vector that has loss as low as possible.

Contributions In this paper, we discuss why considering the loss value at the initial weights alone is not a sufficient criterion for selecting initialization strategies, and discuss which other properties are necessary (section 3). Based thereon, we present a novel initialization strategy that keeps the simplicity of OvAP, but incorporates information about the positive instances for each label to find even better initial weights (section 4). We extend the empirical evaluation of Fang et al. [12] to cover larger datasets with up to 3 million labels, and demonstrate that the proposed method works for both sparse and dense feature spaces (section 5).

We show that, when employed in conjunction with the squared-hinge loss function, the benefit of this initialization is not limited to just starting closer to the final weight vector, but also leads to much faster computations in each training step because of the implicit negative mining. In the converse, we present an example where a certain choice of initial vector provides a decrease of initial loss by several orders of magnitude, but still results in no significant improvement in training time.

2 Conjugate-Gradient Newton Optimization

Setup We are given a dataset $\mathcal{D} = \{(\mathbf{x}_i, \mathbf{y}_i) : i \in [n]\}$ with $n := |\mathcal{X}|$ training instance $\mathbf{x} \in \mathcal{X} = \mathbb{R}^d$ and their corresponding labels $\mathbf{y} \in \mathcal{Y} = \{-1, 1\}^l$. For a label $j \in [l]$ we denote with $\mathcal{P}(j) := \{\mathbf{x}_i : y_{ij} = 1\}$ the instances for which the label is relevant, and analogously $\mathcal{N}(j) = \mathcal{X} \setminus \mathcal{P}(j)$, where $\mathcal{X} := \{\mathbf{x}_i : i \in [n]\}$ is the set of all training instances. This corresponds to a weight vector $\mathbf{y}^{(j)}$ which has entries 1 for each positive instance, $y_i^{(j)} = 1 \Leftrightarrow i \in \mathcal{P}(j)$.

We assume that the number of labels l is large enough that a preprocessing step of $O(n)$ does not disrupt the computational budget, and that the labels are sparse, in the sense that for most $j \in [l]$ we have $|\mathcal{P}(j)| \ll |\mathcal{N}(j)|$. These assumptions are part of what characterizes an XMC problem.

The goal is to find a weight vector \mathbf{w}_j^* for each label $j \in [l]$ that minimizes the risk of the corresponding binary problem with some convex margin loss ϕ , combined with a regularizer \mathcal{R} :

$$\mathcal{L}[\mathbf{w}, \mathbf{y}^{(j)}] := \sum_{i=1}^n \phi(y_i^{(j)} \mathbf{w}^\top \mathbf{x}_i) \quad (3)$$

$$\mathbf{w}_j^* := \mathbf{w}^*(\mathbf{X}, \mathbf{y}^{(j)}) := \underset{\mathbf{w}}{\operatorname{argmin}} \mathcal{L}[\mathbf{w}, \mathbf{y}^{(j)}] + \mathcal{R}[\mathbf{w}]. \quad (4)$$

Throughout this paper, we have used the L_2 norm as the regularizer. From hereon out we will drop the superscript $\mathbf{y}^{(j)}$ and write \mathbf{y} for the vector of labels values for a given label.

Optimization Step The minimization is carried out using a CG Newton procedure inspired by Liblinear [11, 13]. There, a descent direction \mathbf{p} is determined by minimizing a locally-quadratic approximation $\hat{\mathcal{L}}$ to the loss function

$$\hat{\mathcal{L}}(\mathbf{w} + \delta \mathbf{w}) = \mathcal{L}(\mathbf{w}) + \nabla \mathcal{L} \cdot \delta \mathbf{w} + \frac{1}{2} \delta \mathbf{w}^\top \mathbf{H} \delta \mathbf{w}, \quad (5)$$

where \mathbf{H} denotes the Hessian. Then a line-search using a backtracking approach is carried out over $\mathbf{w} + \lambda \mathbf{p}$, $\lambda \in (0, 1]$. The search direction \mathbf{p} can be determined efficiently using CG procedure, as that does not need the full Hessian, but only Hessian-vector products which can be calculated as [18]

$$\mathbf{H} \mathbf{d} = \sum_{i=1}^n \phi''(\mathbf{x}_i^\top \mathbf{w} \cdot y_i) y_i \langle \mathbf{x}_i, \mathbf{d} \rangle \cdot \mathbf{x}_i. \quad (6)$$

Squared Hinge Loss As the margin loss ϕ we use the squared hinge loss (following e.g. [17, 4, 3])

$$\phi(m) = \max(0, 1 - m)^2. \quad (7)$$

Even though this function's second derivative does not exist at $m = 1$, it can be used for second-order optimization [13]. Its hinge structure means that for $m > 1$ we have $\phi(m) = \phi'(m) = \phi''(m) = 0$, which implies that the sum over all data points can be replaced with a sum over implicitly-mined hard instances $\mathcal{A} = \{i : \mathbf{x}_i^\top \mathbf{w} \cdot y_i < 1\}$ [18],

$$\mathbf{H} \mathbf{d} = \sum_{i \in \mathcal{A}} \phi''(\mathbf{x}_i^\top \mathbf{w} \cdot y_i) y_i \langle \mathbf{x}_i, \mathbf{d} \rangle \cdot \mathbf{x}_i, \quad (8)$$

which can be computationally much more efficient than the full sum. The active set \mathcal{A} has to be re-calculated after each weight update, but each weight update requires multiple $\mathbf{H} \mathbf{d}$ calculations for the conjugate-gradient procedure.

In order for the CG Newton optimizer to make good progress, the loss \mathcal{L} should be well approximated by its second-order Taylor expansion. As ϕ is piecewise-quadratic, this is fulfilled when m is far from the boundary at $m = 1$. Let the quadratic approximation $\hat{\phi}_{m_0}$ be defined as

$$\hat{\phi}_{m_0}(\delta) = \phi(m_0) + \delta \phi'|_{m_0} + 0.5 \delta^2 \phi''|_{m_0}, \quad (9)$$

then we can calculate the approximation error based on the step size as $e(\delta; m_0) := \hat{\phi}_{m_0}(\delta) - \phi(m_0 + \delta)$. Two examples are shown in Figure 1. For an instance right at the decision boundary, improving the classification margin to exceed one causes the quadratic approximation to over-estimate the true loss value, leading to smaller proposed update vectors \mathbf{p} . On the other hand, for any instance classified with at least margin 1, the quadratic approximation cannot "see" the increased error as the margin shrinks, and may propose overly large steps \mathbf{p} that have to be shrunk using the line search. The practical consequences of this can be seen in the next section.

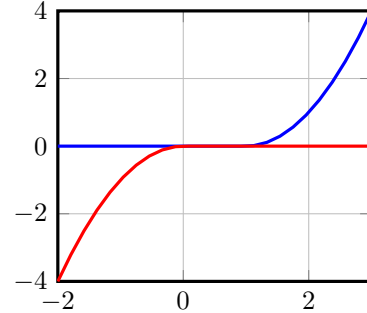


Figure 1: Approximation errors $e(\delta; m_0)$ for $m_0 = 0$ (blue) and $m_0 = 1$ (red) over δ .

3 Analysis of Criteria for Initial Weights

Low Loss as a Criterion for Initial Weights In Fang et al. [12], the authors showed (under some conditions, see their Lemma 3.1) that the optimal weight vector $\mathbf{w}^*(\mathbf{y})$ for one labeling \mathbf{y} results in good performance also for a different labeling \mathbf{y}' if the two label vectors are close in Hamming distance l_H :

$$\mathcal{L}[\mathbf{w}^*(\mathbf{y}), \mathbf{y}'] - \mathcal{L}[\mathbf{w}^*(\mathbf{y}'), \mathbf{y}'] \leq \text{const} \cdot l_H(\mathbf{y}, \mathbf{y}'). \quad (10)$$

Given that for tail labels we have $l_H(\mathbf{y}, -\mathbf{1}) \ll n$, they conclude that using $\mathbf{w}^*(-\mathbf{1})$ makes the initial vector result in much lower loss than using zero-initialized weights. Then, based on convergence rates of iterative minimizers, they estimate the speedup that $\mathbf{w}_0 = \mathbf{w}^*(-\mathbf{1})$ provides over $\mathbf{w}_0 = \mathbf{0}$.

However, this considers only one of the three criteria for fast convergence we listed in the introduction. As we show below, it is entirely possible for an initial vector to induce an initial loss that is orders of magnitude smaller, but still not provide any speedup. The reason is that their estimation is based on asymptotic convergence rates based on the number of iterations. This does not need to agree with actual computation time, for example if the computations become faster closer to the minimum due to implicit negative mining as discussed above.

Furthermore, certain regions in the weight space may be more benign towards the chosen minimization procedure than others. For example, in deep networks one often chooses an initialization procedure that preserves variance and mean over layers, to prevent vanishing or exploding gradients [14]. Such a technique does not provide any reduced loss for the starting point, but is very effective in speeding up the training. For the concrete case of Newton optimization, this means that we require the local quadratic approximation to fit the true loss well, which may become problematic if many points are classified with margin close to 1.

The reason why the method of Fang et al. [12] works well, even though its derivation only considered the reduction in loss, is that as a byproduct it also increases sparsity, and appears to produce vectors that are amenable to Newton optimization. Below, we construct an initialization method that also induces a strong reduction in loss, but does not provide sparsity or useful second-order approximations.

Running Example To evaluate the initialization methods and investigate their properties, we take the AmazonCat-13K dataset from the extreme classification repository [5, 21] as a running example in this section and the next. The input features are sparse tf-idf values of a bag-of-words representation augmented by an additional bias feature that is set to 1. The train/test split is taken from the repository.

Bias-Initialization A simple way to calculate an approximation to $\mathbf{w}^*(-\mathbf{1})$, the optimal weight-vector that predicts the absence of the label for every instance, is to use a weight vector $\mathbf{w}_b = (-1, 0, \dots)^T$, where we assume that the bias feature is at index 0.¹

Then, the score for any instance \mathbf{x} will be $m = -1$, which means that it is classified as negative with margin one, so this weight vector is a minimizer of the squared hinge loss (without regularization). As can be seen in Figure 2 (left), the initial value of the loss is decreased by three orders of magnitude, in fact to a lower value than with the ovap initializer. Yet after some iterations, the ovap based optimization overtakes bias. In particular, the bias-initialized optimization does not make any substantial progress during the first iteration.

This can be explained by the fact that by choosing -1 for the bias weight, the initial weights are exactly at a position where there is a discontinuity in the Hessian. This suggests that it might be beneficial to use a different value for the bias, e.g. $\mathbf{w}_0 = 0.9\mathbf{w}_b$ or $\mathbf{w}_0 = 2\mathbf{w}_b$. This intuition is confirmed by Figure 2 (right), where we can see that both variations make significant progress in the first iteration, with $2\mathbf{w}_b$ clearly outperforming \mathbf{w}_b .

So far, we only have looked at the optimization time in terms of number of iterations, but what we really care about is wall-clock time. Here, the difference between the three bias-init variations becomes even more pronounced. For $2\mathbf{w}_b$ we get 558 seconds, much faster than \mathbf{w}_b and $0.9\mathbf{w}_b$ at 1161 and 995 seconds. This is because the calculations of Hessian-vector products become sparse,

¹Such a strategy seems to have been considered by Fang et al. [12], as it can be found in their code at <https://github.com/fanghgit/XMC>, though it is not mentioned in the paper.

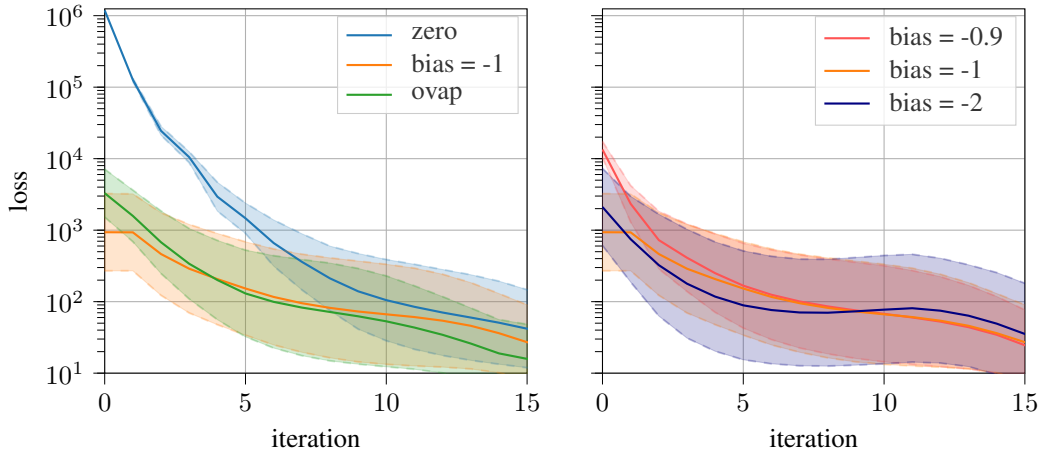


Figure 2: Objective value at different iterations for starting with zero vector, ovap and with bias-initialization \mathbf{w}_b . The right side shows the progress for different values of the bias weight. The shaded area spans the 5% to 95% quantiles. Note that the slight increase in objective for the later iterations is just an artifact due to the fact that we plot the loss values averaged for the binary sub-problems that have not yet terminated at the given iteration. The sub-problems with low loss value terminate earlier, causing an increase in average of the remaining trajectories.

as only those instances with non-zero loss need to be taken into account. For $\lambda \mathbf{w}_b$, $\lambda \geq 1$, these are all the negatives N . However, for $\lambda = 1$ the very first optimization step destroys the sparsity, so even though the first iteration is fast, it does not make progress and makes the following iterations slow again. To a much lesser degree, this also happens for $\lambda = 2$ as can be seen from Figure 4. For $\lambda < 1$, we are not at the discontinuity of the Hessian, but the quadratic approximation now pessimized the actual loss function, and there is no sparsity in the first iteration.

OvA-Primal When running the experiments with the OvA-primal initial vector, we noticed that the choice of stopping criterion for learning the initial vector can have a strong influence on performance. In particular, if we use a criterion as strict as for the actual binary problems, the training time is much larger than for a loose stopping criterion. This can be explained by the fact that the OvA-primal task will converge to a solution with similar characteristics as \mathbf{w}_b , i.e. each training instance will be close to the decision boundary. For the main paper, we have used a stopping criterion of $\|\nabla \mathcal{L}[\mathbf{w}^*]\| \leq 0.01 \|\nabla \mathcal{L}[\mathbf{0}]\|$.

A more detailed discussion of the training dynamics with bias and OvA-primal initialization can be found in the supplementary.

4 Average-of-Positives Initialization

Motivation In this section, we derive a simple way to generate an initial vector which is motivated by the following observation: If the data is linearly separable with margin, then the final weight vector will separate the convex hull of the negatives N from the positives P , which in particular implies that it separates the centres of mass $\bar{\mathbf{p}}$ of the positives and $\bar{\mathbf{n}}$ of the negatives. This means that we can restrict the search space of weight vectors to those that separate $\bar{\mathbf{p}}$ and $\bar{\mathbf{n}}$. A sketch of this situation is given in Figure 3.

Derivation Without making use of any additional information about the training data (as we want a computationally cheap procedure), there are only very general conditions we can impose to choose among these hyperplanes. As a first step, we can parameterize the search space, based on the margins of $\bar{\mathbf{p}}$ and $\bar{\mathbf{n}}$, that is we impose

$$\langle \mathbf{w}_0, \bar{\mathbf{p}} \rangle = s, \quad \langle \mathbf{w}_0, \bar{\mathbf{n}} \rangle = t, \quad (11)$$

for two hyperparameters s and t .

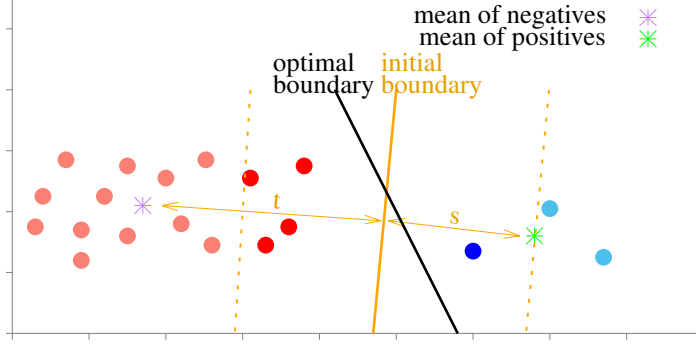


Figure 3: Motivation for the Average-of-Positives initialization. If the data is linearly separable, then the feature-means of the positives (blue) and the negatives (red) will lie on the correct side of the optimal separating hyperplane (black line). Thus we may restrict our search for the initial vector to the set of the separating planes of $\bar{\mathbf{p}}$ and $\bar{\mathbf{n}}$ (orange), which have to lie in the plane spanned by $\bar{\mathbf{p}}$ and $\bar{\mathbf{n}}$ if we want a minimum-norm solution. In order to achieve strong implicit negative mining in the first epoch, we choose a solution where the center of mass of the negatives is classified correctly with a large margin (dashed orange lines), so that most of the negatives (light red) will be classified correctly with a margin over more than 1 and thus not enter the Hessian computation.

These are only two linear constraints in the high dimensional weight space. However, for good generalization, we prefer weight vectors with minimal norm. If we want a minimum L_2 -norm solution, then the search space becomes restricted to $\text{span}(\bar{\mathbf{p}}, \bar{\mathbf{n}})$, and we can parameterize $\mathbf{w}_0 = u\bar{\mathbf{p}} + v\bar{\mathbf{n}}$. This leads to a system of two linear equations in the two unknowns u and v , with a unique solution except in the unlikely event that $\bar{\mathbf{p}}$ and $\bar{\mathbf{n}}$ are linearly dependent.

Reparameterization for Efficiency Since most labels have only few positive instances, their mean $\bar{\mathbf{p}}$ can be calculated quickly, but calculating $\bar{\mathbf{n}}$ directly would be an $O(n)$ operation. However, we can precompute the mean of all instances $\bar{\mathbf{x}}$, and use the property

$$|\mathbf{N}|\bar{\mathbf{n}} + |\mathbf{P}|\bar{\mathbf{p}} = |\mathbf{X}|\bar{\mathbf{x}}. \quad (12)$$

Because $\text{span}(\bar{\mathbf{p}}, \bar{\mathbf{n}}) = \text{span}(\bar{\mathbf{p}}, \bar{\mathbf{x}})$, we can make the equivalent parameterization $\mathbf{w}_0 = u\bar{\mathbf{p}} + v\bar{\mathbf{n}}$, leading to the equations

$$s = \langle \mathbf{w}_0, \bar{\mathbf{p}} \rangle = \langle u\bar{\mathbf{p}} + v\bar{\mathbf{x}}, \bar{\mathbf{p}} \rangle = v\langle \bar{\mathbf{x}}, \bar{\mathbf{p}} \rangle + u\langle \bar{\mathbf{p}}, \bar{\mathbf{p}} \rangle \quad (13)$$

$$|\mathbf{N}|t = |\mathbf{N}|\langle \mathbf{w}_0, \bar{\mathbf{n}} \rangle = \langle u\bar{\mathbf{p}} + v\bar{\mathbf{x}}, |\mathbf{X}|\bar{\mathbf{x}} - |\mathbf{P}|\bar{\mathbf{p}} \rangle. \quad (14)$$

Defining $\alpha := |\mathbf{P}|/|\mathbf{X}|$ leads to

$$u = \frac{\langle \bar{\mathbf{x}}, \bar{\mathbf{p}} \rangle (t + (s - t)\alpha) - s\langle \bar{\mathbf{x}}, \bar{\mathbf{x}} \rangle}{\langle \bar{\mathbf{p}}, \bar{\mathbf{x}} \rangle^2 - \langle \bar{\mathbf{p}}, \bar{\mathbf{p}} \rangle \langle \bar{\mathbf{x}}, \bar{\mathbf{x}} \rangle} \quad (15)$$

$$v = (s - u\langle \bar{\mathbf{p}}, \bar{\mathbf{p}} \rangle) / \langle \bar{\mathbf{x}}, \bar{\mathbf{p}} \rangle. \quad (16)$$

A short discussion on the situations if the denominators become zero is given in the supplementary.

As we want the loss vector corresponding to the initial weights to be sparse, we want the distance of $\bar{\mathbf{n}}$ to the decision boundary to be larger than that of $\bar{\mathbf{p}}$. Empirically, we found $s = 1$, $t = -2$ (cf. supplementary) to work well.

Evaluation Does this initialization method work as we expect? As shown in Figure 4, this method induces loss vectors that are a bit more sparse than the ones for ovap, and keep this property over the course of training, inducing faster update times for each iteration. As expected, we get the most benefit for tail labels, where the assumptions of Figure 3 are much better fulfilled than for head labels. Still, our method is faster or at least as fast as any of the other methods across the entire range of number of positives. Additional graphs showing the number of iterations, duration per iteration etc. can be found in the supplementary.

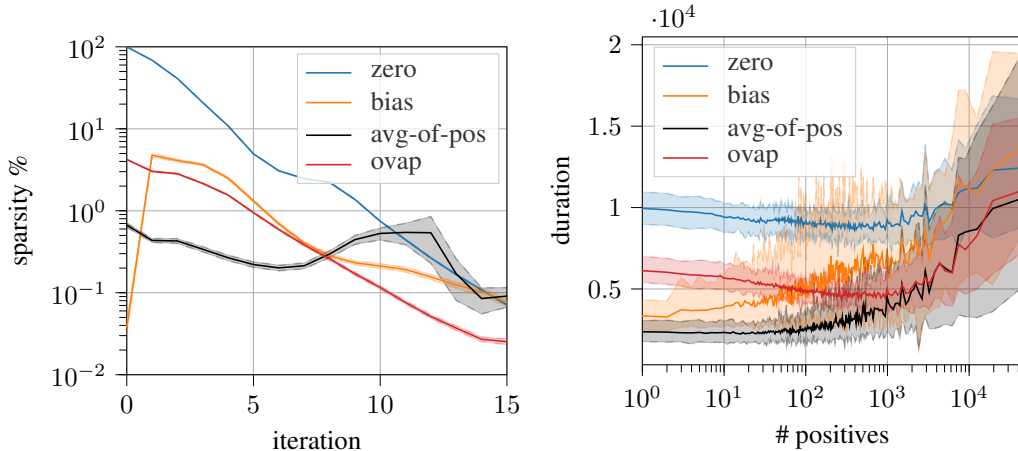


Figure 4: On the left, the sparsity (in percent of nonzeros) of the Hessian calculation over different training epochs is shown. Even though bias-initialization starts out very sparse, this property is lost after the first update step. On the right, the training time for a single label is shown, depending on the number of positives for that label. The shaded area marks the 5% to 95% quantile.

5 Experimental Evaluation

Infrastructure and Training Configuration Our code is a re-implementation of the conjugate-gradient Newton procedure of recent versions of Liblinear [13]. The hyperparameters related to stopping condition for conjugate-gradient iterations ($\epsilon = 0.5$) preconditioner ($\alpha = 0.01$), back-tracking line search ($\alpha = 0.5$, $\eta = 0.01$, $\text{max_steps} = 20$), and stopping condition for the optimization ($\epsilon = 0.01$) have been taken from their code. To reduce model size, all weights below a threshold of 0.01 have been clipped to zero.

All our experiments were run on a single compute node equipped with two AMD Rome 7H12 CPUs. The code is NUMA-aware and produces a copy of the training data for each NUMA-node, but memory bandwidth still is the limiting factor in scalability. We observed very good scaling for 64 cores, but sublinear improvements for more cores. This means that the reported times here cannot be directly converted to single-core timings by multiplying with 128.

Sparse Data We ran tests using the Eurlex-3k [25], AmazonCat-13k [21], WikiSeeAlsoTitles-350K, WikiTitles-500k, Amazon-670k [21], WikiLSHTC-325k [28], Amazon-3M [23, 22], and Wikipedia-500k [5] in their train/test splits as available from Bhatia et al. [5]. For the latter dataset, we could not train the model within the 36 hour job time limit on our cluster system, even with the improved initialization. For Amazon-3M we have only run our initializer due to the large computational cost involved, so we cannot report the speed-up, but we have demonstrated that learning a DiSMEC-style model is feasible even for datasets with more than a million labels.

As shown in Table 1, our method is 3 to 4 times faster than zero initialization, and also significantly faster than bias and ovap initialization. Based on the timing reported in Fang et al. [12], we have also calculated the speedup of the OvA-Primal++ method introduced there, for the datasets for which they have run tests.

Because the optimization problem is convex, the minimum is not affected by the choice of initial parameter. However, because in practice only an approximate minimum is found, there are slight variations (around 0.1%) in precision@k metrics for the different methods. The concrete numbers can be found in the supplementary.

Dense Data We also ran the tests on the same dataset of dense features as used for slice ². We noticed that the default setting for the stopping condition as specified by Liblinear, $\epsilon = 0.01$, is far

²<http://manikvarma.org/code/Slice/download.html>

Table 1: Training time for different datasets and initialization methods. *The timings are given in minutes.* For the logistic loss, we have changed to $t = -3$. Ratio denotes the time taken with zero-initialization divided by aop-initialization, the ovap++ column is the relative speedup of the spanning-tree based OvA-Primal++ method, calculated from the values reported in Fang et al. [12].

Dataset	Setting	zero	bias	aop	ovap	Ratio	ovap++
Eurlex-4k	tf-idf	0.18	0.13	0.10	0.12	1.8	1.9
Amazoncat-13k	tf-idf	17.48	9.28	5.80	10.67	3.0	1.8
Amazoncat-14k	tf-idf	76.05	29.83	20.28	41.62	3.7	2.1
Wiki10-31k	tf-idf	3.98	3.58	2.35	3.15	1.7	1.8
WikiLSHTC	tf-idf	1,110.96	479.46	310.45	687.94	3.6	—
WikiTitles-500k	tf-idf	292.64	93.30	71.83	315.32	4.1	—
Amazon-670k	tf-idf	317.09	148.76	84.08	197.33	3.8	—
Amazon-3M	tf-idf	—	—	1,162.85	—	—	—
Eurlex-4k	slice	0.13	0.07	0.05	0.07	2.7	—
Amazon-670k	slice	782.39	376.47	321.19	489.15	2.4	—
Amazoncat-13k	logistic	29.30	25.28	23.50	20.23	1.3	—

too strict in this setting. Therefore, we’ve increased this parameter for $\epsilon = 1$ here. For these settings, we observed larger variability in the classification accuracy.

Logistic Loss We have also run a test where we replaced the squared hinge loss with the logistic loss. As the logistic loss only vanishes asymptotically, this is a setting where we cannot benefit from implicit negative mining. This means that later iterations will take approximately as long as earlier ones, and there is much less benefit from being able to skip the first iterations. The result is a much reduced benefit from our proposed initialization.

Due to the vast number of negatives (for a tail label), the loss function’s minimum will not be achieved when the negatives are classified correctly with margin one as is the case with squared-hinge, but will in fact train a larger margin for the negatives. This suggests that by decreasing the t parameter further, our initial guess for the separating hyperplane will be closer to the truth.

6 Discussion

We have provided a way to initialize the weights of a linear OvA extreme classifier in such a way as to reduce training times. Our experiments show that aside from the initial loss value investigated in Fang et al. [12], the implicit sparsity and local smoothness properties of the loss landscape also play an important role in the success of the method.

Outlook The choice of initial vector is an underexplored design tool in XMC that is orthogonal to many other design choices such as explicit negative mining [32, 17], training meta classifiers over buckets of labels [24, 7], or the choice of regularizer. Future work should thus look into combining these, for example integrating our initialization into the OvA parts of Slice[17], Parabel [30], Probabilistic Label Trees [35], or Astec [7].

Limitations The initialization method discussed in this work is mainly applicable to linear one-vs-rest XMC algorithms. This rules out label-embedding schemes [16, 6], decision-tree based classifiers [29, 20] and deep-learning methods in which the classifier is jointly learnt with the intermediate representations [37].

Acknowledgments and Disclosure of Funding

We wish to acknowledge CSC – IT Center for Science, Finland, as well as the Aalto Science-IT project, for providing the required computational resources. We would also like to thank Mohammadreza Qaraei for his help in preparing Figure 3.

References

- [1] Lada A Adamic and Bernardo A Huberman. “Zipf’s law and the Internet.” In: *Glottometrics* 3.1 (2002), pp. 143–150.
- [2] Rahul Agrawal et al. “Multi-Label Learning with Millions of Labels: Recommending Advertiser Bid Phrases for Web Pages”. In: *Proceedings of the 22nd International Conference on World Wide Web. WWW ’13*. Rio de Janeiro, Brazil: Association for Computing Machinery, 2013, pp. 13–24.
- [3] Rohit Babbar and Bernhard Schölkopf. “Data scarcity, robustness and extreme multi-label classification”. In: *Machine Learning* 108.8 (2019), pp. 1329–1351.
- [4] Rohit Babbar and Bernhard Schölkopf. “DiSMEC: Distributed Sparse Machines for Extreme Multi-Label Classification”. In: *Proceedings of the Tenth ACM International Conference on Web Search and Data Mining. WSDM ’17*. Cambridge, United Kingdom: Association for Computing Machinery, 2017, pp. 721–729.
- [5] K. Bhatia et al. *The extreme classification repository: Multi-label datasets and code*. 2016. URL: <http://manikvarma.org/downloads/XC/XMLRepository.html>.
- [6] Kush Bhatia et al. “Sparse Local Embeddings for Extreme Multi-label Classification.” In: *NIPS*. Vol. 29. 2015, pp. 730–738.
- [7] Kunal Dahiya et al. “DeepXML: A Deep Extreme Multi-Label Learning Framework Applied to Short Text Documents”. In: *Proceedings of the 14th ACM International Conference on Web Search and Data Mining*. 2021, pp. 31–39.
- [8] Ofer Dekel and Ohad Shamir. “Multiclass-Multilabel Classification with More Classes than Examples”. In: *Proceedings of the Thirteenth International Conference on Artificial Intelligence and Statistics*. Ed. by Yee Whye Teh and Mike Titterton. Vol. 9. Proceedings of Machine Learning Research. Chia Laguna Resort, Sardinia, Italy: PMLR, May 2010, pp. 137–144.
- [9] Jia Deng et al. “What does classifying more than 10,000 image categories tell us?” In: *ECCV*. 2010.
- [10] John Duchi, Elad Hazan, and Yoram Singer. “Adaptive Subgradient Methods for Online Learning and Stochastic Optimization”. In: *Journal of Machine Learning Research* 12.61 (2011), pp. 2121–2159.
- [11] Rong-En Fan et al. “LIBLINEAR: A library for large linear classification”. In: *the Journal of machine Learning research* 9 (2008), pp. 1871–1874.
- [12] Huang Fang et al. “Fast training for large-scale one-versus-all linear classifiers using tree-structured initialization”. In: *Proceedings of the 2019 SIAM International Conference on Data Mining*. SIAM. 2019, pp. 280–288.
- [13] Leonardo Galli and Chih-Jen Lin. “A Study on Truncated Newton Methods for Linear Classification”. In: *IEEE Transactions on Neural Networks and Learning Systems* (2021).
- [14] Xavier Glorot and Yoshua Bengio. “Understanding the difficulty of training deep feedforward neural networks”. In: *Proceedings of the thirteenth international conference on artificial intelligence and statistics. JMLR Workshop and Conference Proceedings*. 2010, pp. 249–256.
- [15] Priya Goyal et al. *Accurate, Large Minibatch SGD: Training ImageNet in 1 Hour*. 2018. arXiv: 1706.02677 [cs.LG].
- [16] Chuan Guo et al. “Breaking the Glass Ceiling for Embedding-Based Classifiers for Large Output Spaces”. In: *Advances in Neural Information Processing Systems*. Ed. by H. Wallach et al. Vol. 32. Curran Associates, Inc., 2019.
- [17] Himanshu Jain et al. “Slice: Scalable linear extreme classifiers trained on 100 million labels for related searches”. In: *WSDM*. 2019, pp. 528–536.
- [18] S Sathya Keerthi, Dennis DeCoste, and Thorsten Joachims. “A modified finite Newton method for fast solution of large scale linear SVMs.” In: *Journal of Machine Learning Research* 6.3 (2005).
- [19] J. Liu et al. “Deep Learning for Extreme Multi-label Text Classification”. In: *Proceedings of the 40th International ACM SIGIR Conference on Research and Development in Information Retrieval* (2017).
- [20] Maryam Majzoubi and Anna Choromanska. “Ldsm: Logarithm-depth streaming multi-label decision trees”. In: *International Conference on Artificial Intelligence and Statistics*. PMLR. 2020, pp. 4247–4257.

- [21] Julian McAuley and Jure Leskovec. “Hidden factors and hidden topics: understanding rating dimensions with review text”. In: *Proceedings of the 7th ACM conference on Recommender systems*. 2013, pp. 165–172.
- [22] Julian McAuley, Rahul Pandey, and Jure Leskovec. “Inferring networks of substitutable and complementary products”. In: *Proceedings of the 21th ACM SIGKDD international conference on knowledge discovery and data mining*. 2015, pp. 785–794.
- [23] Julian McAuley et al. “Image-based recommendations on styles and substitutes”. In: *Proceedings of the 38th international ACM SIGIR conference on research and development in information retrieval*. 2015, pp. 43–52.
- [24] Tharun Medini et al. “Extreme classification in log memory using count-min sketch: A case study of amazon search with 50m products”. In: *arXiv preprint arXiv:1910.13830* (2019).
- [25] Eneldo Loza Mencía and Johannes Fürnkranz. “Efficient pairwise multilabel classification for large-scale problems in the legal domain”. In: *Joint European Conference on Machine Learning and Knowledge Discovery in Databases*. Springer. 2008, pp. 50–65.
- [26] Tomas Mikolov et al. “Efficient estimation of word representations in vector space”. In: *arXiv preprint arXiv:1301.3781* (2013).
- [27] Andriy Mnih and Geoffrey E Hinton. “A Scalable Hierarchical Distributed Language Model”. In: *Advances in Neural Information Processing Systems*. Ed. by D. Koller et al. Vol. 21. Curran Associates, Inc., 2009.
- [28] Ioannis Partalas et al. “Lshc: A benchmark for large-scale text classification”. In: *arXiv preprint arXiv:1503.08581* (2015).
- [29] Yashoteja Prabhu and Manik Varma. “Fastxml: A fast, accurate and stable tree-classifier for extreme multi-label learning”. In: *Proceedings of the 20th ACM SIGKDD international conference on Knowledge discovery and data mining*. 2014, pp. 263–272.
- [30] Yashoteja Prabhu et al. “Parabel: Partitioned label trees for extreme classification with application to dynamic search advertising”. In: *Proceedings of the 2018 World Wide Web Conference*. 2018, pp. 993–1002.
- [31] Mohammadreza Qaraei et al. “Convex Surrogates for Unbiased Loss Functions in Extreme Classification With Missing Labels”. In: *Proceedings of The Web Conference 2021*. WWW ’21. Ljubljana, Slovenia: Association for Computing Machinery, 2021.
- [32] Sashank J Reddi et al. “Stochastic negative mining for learning with large output spaces”. In: *The 22nd International Conference on Artificial Intelligence and Statistics*. PMLR. 2019, pp. 1940–1949.
- [33] Sebastian Ruder. *An overview of gradient descent optimization algorithms*. 2017. arXiv: 1609.04747 [cs.LG].
- [34] Leslie N Smith. “Cyclical learning rates for training neural networks”. In: *2017 IEEE winter conference on applications of computer vision (WACV)*. IEEE. 2017, pp. 464–472.
- [35] Marek Wydmuch et al. “A no-regret generalization of hierarchical softmax to extreme multi-label classification”. In: *Advances in Neural Information Processing Systems 31*. Ed. by S. Bengio et al. Curran Associates, Inc., 2018, pp. 6355–6366.
- [36] Ian EH Yen et al. “Ppdspare: A parallel primal-dual sparse method for extreme classification”. In: *Proceedings of the 23rd ACM SIGKDD International Conference on Knowledge Discovery and Data Mining*. 2017, pp. 545–553.
- [37] Ronghui You et al. “AttentionXML: Label Tree-based Attention-Aware Deep Model for High-Performance Extreme Multi-Label Text Classification”. In: *Advances in Neural Information Processing Systems*. Ed. by H. Wallach et al. Vol. 32. Curran Associates, Inc., 2019.

7 Supplementary

7.1 What happens if the denominator of aop is zero

The expression in equation (15) diverges if $\bar{\mathbf{p}}$ and $\bar{\mathbf{x}}$ are linearly dependent, which implies that the means of features for negatives and positives only differs by a factor. In that case, we cannot (except in unlikely special cases) find an initial vector that fulfills our condition, so we return the zero vector.

A second numerical instability occurs if $|\langle \bar{\mathbf{x}}, \bar{\mathbf{p}} \rangle| \ll 1$, during the calculation of v . To investigate this setting, we substitute $\langle \bar{\mathbf{x}}, \bar{\mathbf{p}} \rangle$ with 0 in (15) and (16).

$$s = u \langle \bar{\mathbf{p}}, \bar{\mathbf{p}} \rangle \quad (17)$$

$$|N|t = v|X| \langle \bar{\mathbf{x}}, \bar{\mathbf{x}} \rangle - u|P| \langle \bar{\mathbf{p}}, \bar{\mathbf{p}} \rangle \quad (18)$$

This leads to

$$u = \frac{s}{\langle \bar{\mathbf{p}}, \bar{\mathbf{p}} \rangle}, \quad v = \frac{|N|t + |P|s}{|X| \langle \bar{\mathbf{x}}, \bar{\mathbf{x}} \rangle}. \quad (19)$$

7.2 Additional graphs for training with bias initialization

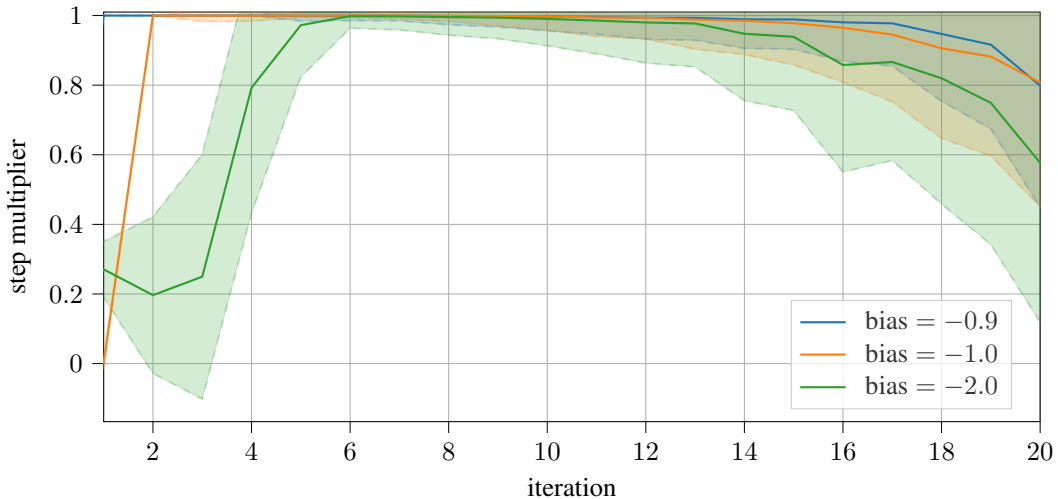


Figure 5: Multiplier found by backtracking line search, i.e. the fraction of the descent direction as found by the CG solver that can be applied to the real objective function and still lead to sufficient reduction in loss. The shaded area indicates \pm one standard deviation. Having a value smaller than one indicates that the quadratic approximation to the loss is overly optimistic in the given direction, and the real step has to be scaled down. As discussed in the main text (Figure 1), this happens when the direction in question is such that it reduces the margin of an instance that is classified correctly with margin more than one. This effect can be seen in the graph here:

For bias = -0.9 , all the negative instances still have nonzero error, so the update will choose a direction that makes them more negative, which is a direction in which the quadratic approximation is overestimating the loss.

On the other hand, with bias = -1 , the only nonzero signal is coming from the positive instances, which will cause the bias to be reduced. Thus, most of the negative instances will get nonzero error, and the quadratic approximation severely underestimates the true loss. Consequently, the line search shows that only a minute step towards the desired direction is allowed.

For bias = -2 , the situation is similar, but this time the distance for each negative instance until it gets nonzero error is much larger, and as such the underestimation effect is reduced and larger stepsize multipliers are possible.

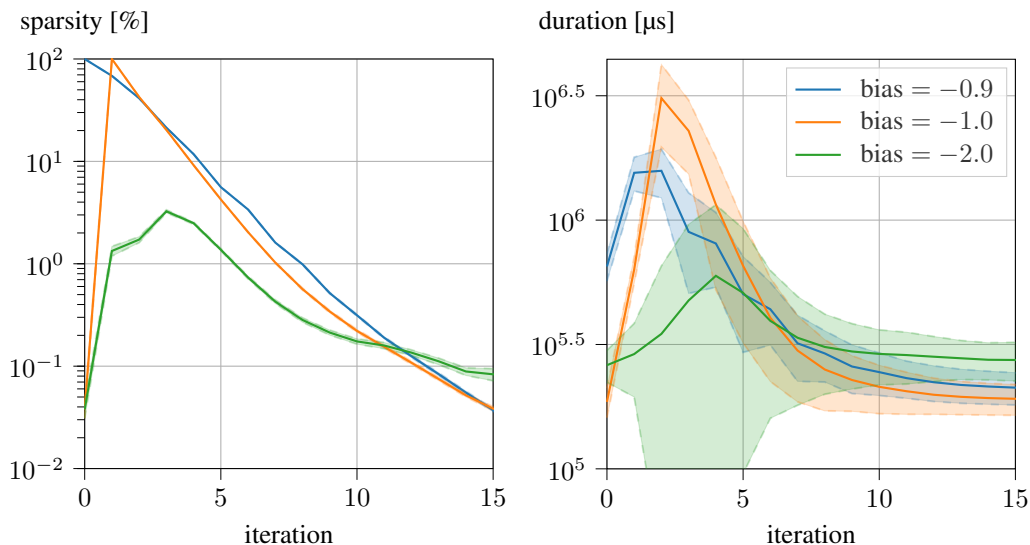


Figure 6: The average sparsity (in percent of nonzeros) and corresponding duration (in μs) of one iteration of the Newton optimization. The averages are taken over the individual binary problems, and the shaded area shows the 2σ error of the mean. The total computation time includes a (sparse) matrix multiplication and a varying number of CG steps. As this data shows, even though -1 and -2 start very sparse, much of the sparsity is lost during the first training steps. For the later iterations, -2 results in slightly less sparsity and slower iterations, however the effect on total running time is far overshadowed by the much faster earlier iterations (note the logarithmic axes). As Figure 7 shows that bias = -2 finishes after at most 15 steps, this graph also indicates that the approximate minima found by the different initialization procedures have slightly different characteristics: The larger sparsity in -0.9 and -1.0 setting means that fewer instances need to have a larger contribution to the overall error.

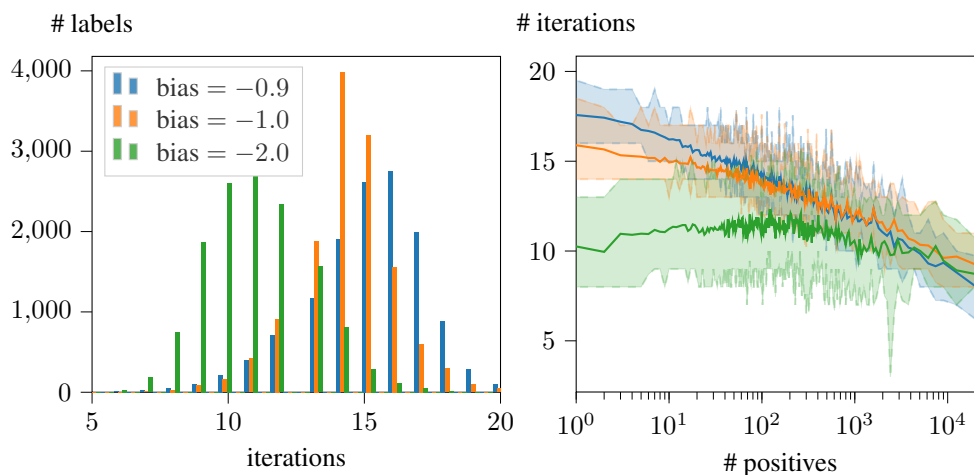


Figure 7: Number of Newton optimization steps required for convergence. On the left, the data is shown as a histogram, with the bins corresponding to the number of binary problems that required the corresponding number of steps. On the right, the average number of steps, and the 95% quantiles, are plotted as a function of the number of positive instances. The data shows that the benefit of the bias = -2 initialization is not limited purely to faster iterations because of increased sparsity, but it also needs fewer steps, despite having slightly larger initial loss than bias = -1 . This indicates that each step has to make more progress, i.e. the loss landscape is more benign to the Newton optimization around the bias = -2 trajectory. The right-hand graph also shows that most of the benefit comes from the tail labels.

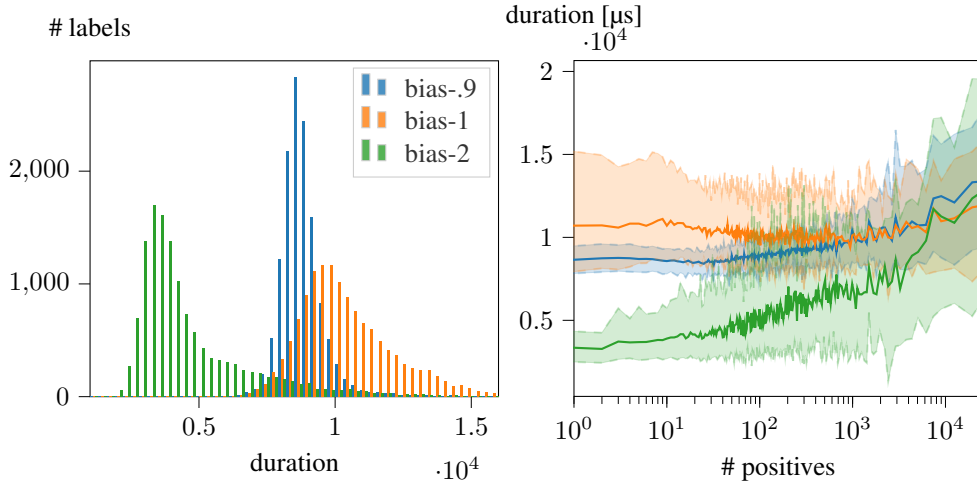


Figure 8: Total duration of the individual binary problems. The histogram on the left has bins corresponding to the number of binary problems taking a certain amount of time, on the right the average time and 95% quantiles are shown in dependence of the number of positive instances. Duration is measured in milliseconds. The graphs show that bias = -1 is a local maximum in terms of computation time.

7.3 Additional graphs for training with ovap initialization

The two figures in this section justify our choice of using a loose stopping criterion for the ovap baseline in the main part of the paper. A more strict criterion leads to lower initial loss, but results in weights unfavourable for the Newton optimizer Figure 9. As a consequence, the strict convergence initial vector leads to overall slower training, as shown in Figure 10.

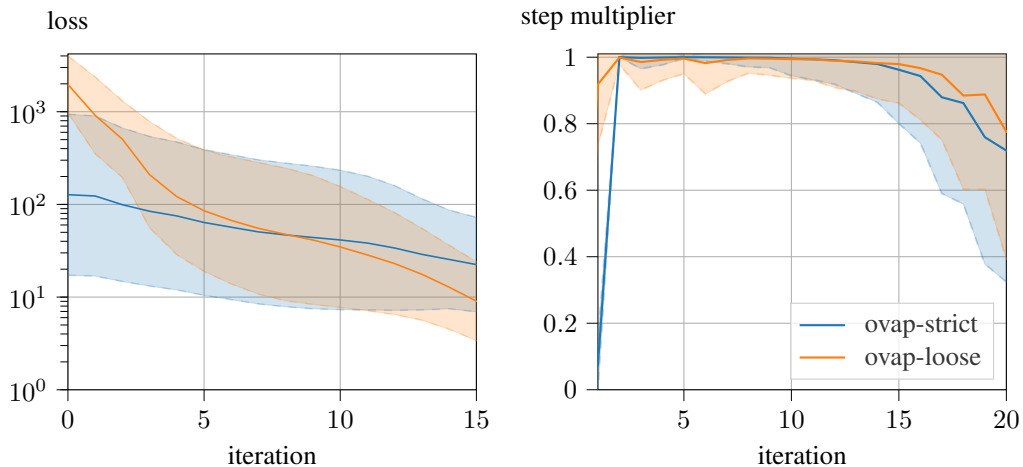


Figure 9: Letting the OvA-Primal initial vector be the result of training the all-zero-label problem until convergence (strict) results in much worse performance than doing early stopping (loose). We suspect that this is because strict training brings the weight vectors into a regime that is qualitatively similar to the bias = -1 setting: All training instances will predict a negative label with a margin very close to 1. Even though this results in much lower initial loss (left), it also leads to a useless first iteration in which little progress is made (right).

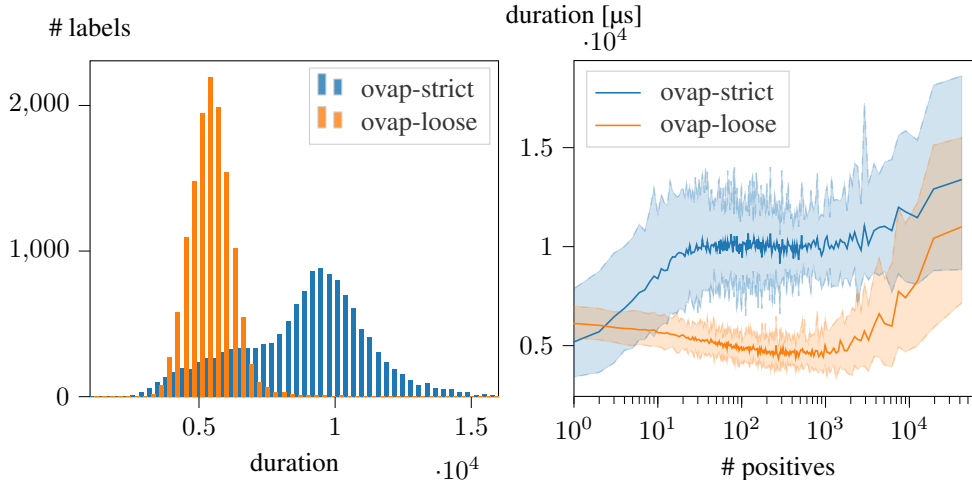


Figure 10: Histogram (left) and average with 95% confidence interval in dependence of the number of positive instance (right) of the training time, measured in milliseconds. Overall, the `loose` training configuration is much faster, though for extreme tail labels with less than 3 positive instances, `strict` actually performs slightly better.

7.4 Choice of hyperparameters for aop

As argued in the main text, in order to achieve sparsity in the Hessian calculations, having the average of the negative instances be classified very strongly as a negative would be beneficial. Interestingly, Figure 11 shows not only the expected speedup in per-iteration time, but also that $t = -1$ requires significantly more iterations than the other two settings.

This is not too surprising, given that we expect that the large number of negative instances fill a larger proportion of the space than the few positives, so the separating hyperplane should be closer to the mean of the positives. One reason for this could be that $t = -1$ induces a higher initial loss than the other two settings, as shown in the bottom left graph. However, if we measure the distance that the optimization procedure covers, i.e. the distance between the initial and final weight vector, it turns out that $t = -1$ actually starts closest.

7.5 Additional graphs for comparing the methods

As shown in Figure 12, using the `aop` initialization drastically reduces the number of iterations needed for convergence for tail labels. Whereas for zero and `ovap` initialization the number of iterations increases as the number of positive instances decreases whereas for `bias` and `aop` initialization it remains almost constant. This cannot be explained by looking only at the distance the optimization algorithm has to travel, neither in terms of the initial loss value, nor in terms of the distance between initial and final weight vector. In Figure 13 we see that these values are much lower for tail labels (except for zero init).

In Figure 14 the duration of a single iteration, and the step size multiplier of the backtracking line search are presented.

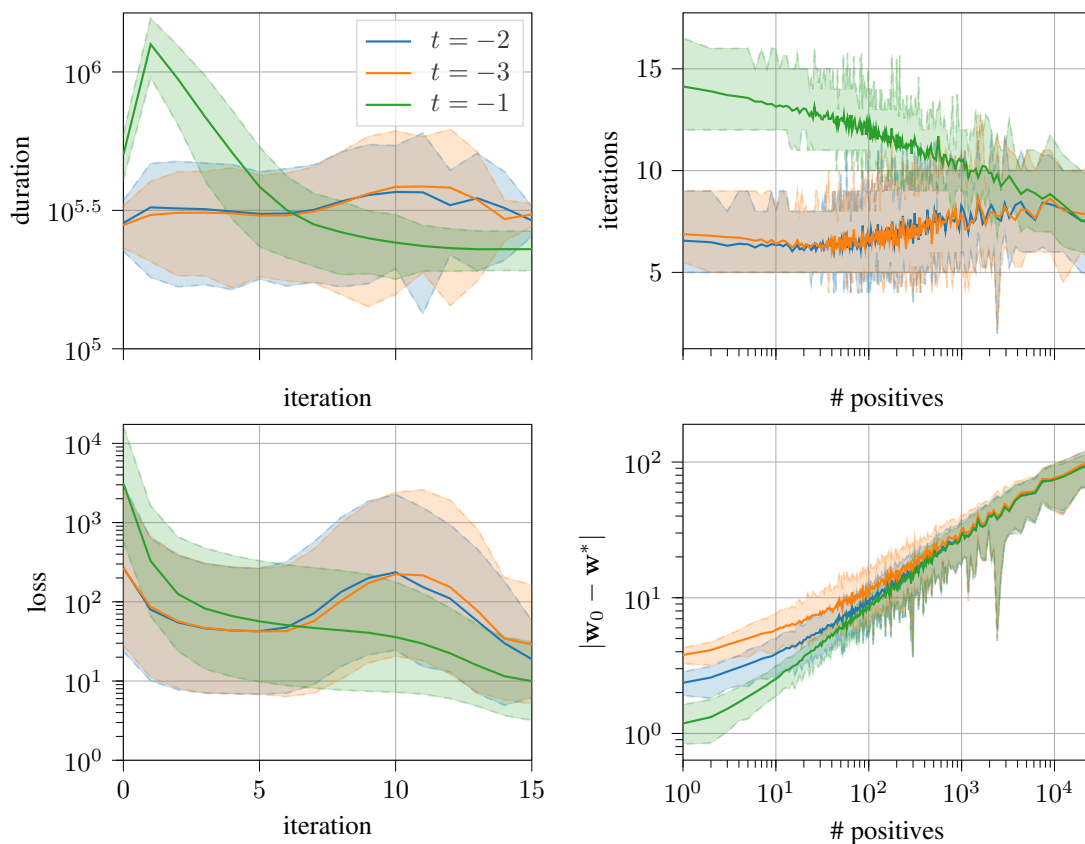


Figure 11: Average duration of the iterations (top left, in μs), and number of iterations for different numbers of positive instances (top right). The bottom left graph shows the development of the objective function. At first glance, this seems paradoxical, as the algorithm is designed so that for each binary problem, the loss strictly decreases over the iterations. The apparent increase is caused by the fact that the sample of binary problems shrinks for later iterations, as the labels for which the loss is already low before will terminate the optimization. Finally, the bottom right graph shows the Euclidean distance between the initial weight vector and the approximately optimal weight vector for which the minimization is terminated. The shaded area marks the 95% quantile.

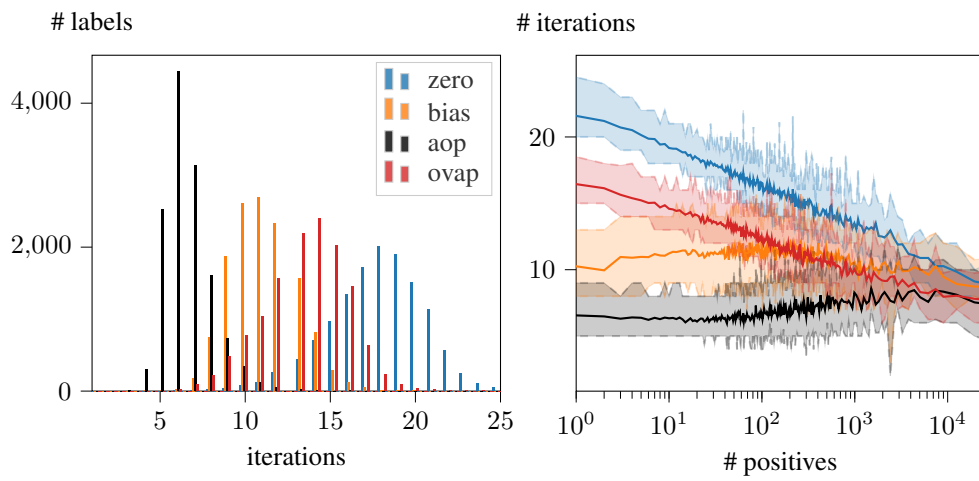


Figure 12: Number of Newton optimization steps required for convergence. On the left, the data is shown as a histogram, with the bins corresponding to the number of binary problems that required the corresponding number of steps. On the right, the average number of steps, and the 95% quantiles, are plotted as a function of the number of positive instances.

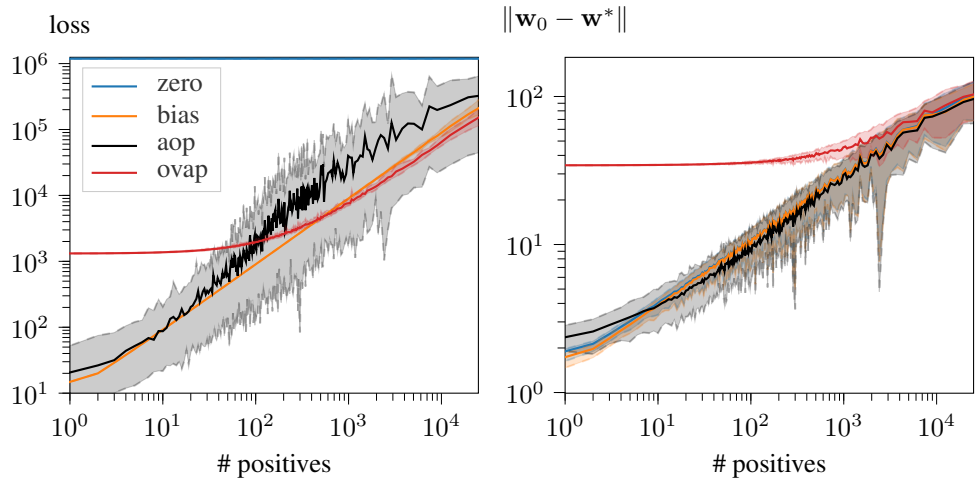


Figure 13: Loss of the initial weight vector (left) and distance between initial and final vector (right). The shaded area shows 95% quantiles. For all except zero initialization, loss and distance are much lower for tail labels than for head labels.

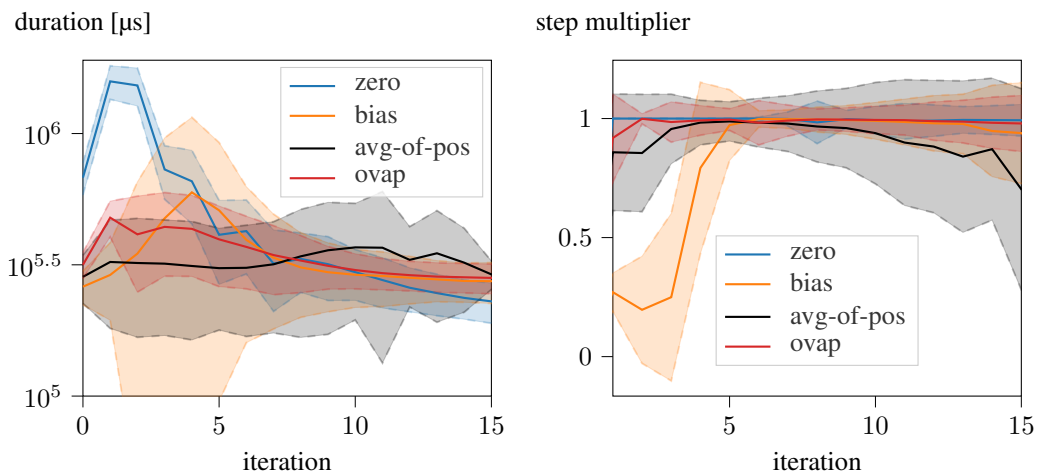


Figure 14: Duration of a single iteration (left), and line search step multiplier (right). The aop initialization manages to have the early iterations as fast as the later ones, while still working much better in terms of the quadratic approximation than the bias initialization. The decrease of the step multiplier for late iterations is not relevant, because as Figure 12 shows most of the binary problems will have finished by iteration 10.

7.6 Full Result Table

Table 2: Durations (as given in main paper) and precision@{1,3,5} for training different datasets with the given initialization methods. Since the actual loss function is based on binary classification, we have also calculated the precision and recall as averaged over the individual binary problems. The metrics remain mostly unchanged for tf-idf data, but there is significant fluctuation when slice features are used. The aop* setting refers to a training run where $t = -3$ was used, which turned out to be beneficial in the logistic loss setting.

Dataset	Setting	Method	P@1	P@3	P@5	Prec	Rec	Duration
Eurlex-4k	tf-idf	zero	82.8	70.3	58.8	80.3	37.6	0.18
Eurlex-4k	tf-idf	bias	82.9	70.4	58.9	80.2	37.6	0.13
Eurlex-4k	tf-idf	aop	82.9	70.4	58.9	80.3	37.6	0.10
Eurlex-4k	tf-idf	ovap	82.9	70.4	58.9	80.3	37.6	0.12
Amazoncat-13k	tf-idf	zero	93.8	79.1	64.1	84.4	58.5	17.48
Amazoncat-13k	tf-idf	bias	93.8	79.1	64.1	84.5	58.4	9.28
Amazoncat-13k	tf-idf	aop	93.7	79.1	64.1	84.4	58.4	5.80
Amazoncat-13k	tf-idf	ovap	93.8	79.1	64.1	84.4	58.5	10.67
Amazoncat-14k	tf-idf	zero	89.9	69.6	54.9	87.1	66.8	76.05
Amazoncat-14k	tf-idf	bias	89.8	69.6	54.9	87.1	66.7	29.83
Amazoncat-14k	tf-idf	aop	89.8	69.6	54.9	87.2	66.6	20.28
Amazoncat-14k	tf-idf	ovap	89.8	69.6	54.9	87.2	66.6	41.62
WikiLSHTC	tf-idf	zero	64.2	42.5	31.5	84.4	19.3	1,110.96
WikiLSHTC	tf-idf	bias	64.1	42.5	31.5	84.5	19.3	479.46
WikiLSHTC	tf-idf	aop	64.2	42.5	31.6	84.4	19.4	310.45
WikiLSHTC	tf-idf	ovap	64.2	42.5	31.5	84.4	19.3	687.94
WikiTitles-500k	tf-idf	zero	39.3	20.8	14.7	66.5	5.3	292.64
WikiTitles-500k	tf-idf	bias	39.3	20.8	14.7	66.6	5.3	93.30
WikiTitles-500k	tf-idf	aop	39.3	20.8	14.7	66.7	5.3	71.83
WikiTitles-500k	tf-idf	ovap	39.3	20.8	14.7	66.5	5.3	315.32
Amazon-670k	tf-idf	zero	44.8	39.7	36.2	79.3	18.7	317.09
Amazon-670k	tf-idf	bias	44.8	39.7	36.1	79.3	18.7	148.76
Amazon-670k	tf-idf	aop	44.8	39.7	36.2	79.3	18.7	84.08
Amazon-670k	tf-idf	ovap	44.7	39.8	36.1	79.3	18.7	197.33
Amazon-670k	slice	zero	35.6	32.1	29.4	74.6	23.0	782.39
Amazon-670k	slice	bias	34.2	31.0	28.5	69.4	22.4	376.02
Amazon-670k	slice	aop	35.6	32.1	29.5	73.5	23.4	321.19
Amazon-670k	slice	ovap	35.6	32.0	29.4	74.5	23.0	489.15
Amazoncat-13k	logistic	zero	93.2	77.5	61.9	85.8	47.2	29.30
Amazoncat-13k	logistic	bias	93.2	77.5	61.8	85.8	47.1	25.28
Amazoncat-13k	logistic	aop	93.2	77.5	61.8	85.8	47.1	25.13
Amazoncat-13k	logistic	ovap	93.1	77.5	61.8	85.8	47.1	20.23
Wiki10-31k	tf-idf	zero	84.1	74.7	66.0	75.7	13.2	3.98
Wiki10-31k	tf-idf	bias	84.2	74.8	66.0	75.7	13.2	3.58
Wiki10-31k	tf-idf	aop	84.2	74.7	66.0	75.6	13.2	2.35
Wiki10-31k	tf-idf	ovap	84.2	74.7	66.0	75.6	13.2	3.15
Eurlex-4k	slice	zero	77.2	63.4	51.3	72.8	36.3	0.13
Eurlex-4k	slice	bias	75.3	62.1	50.2	76.0	26.4	0.07
Eurlex-4k	slice	aop	76.6	63.0	51.4	67.7	39.1	0.05
Eurlex-4k	slice	ovap	76.9	63.5	51.4	72.5	36.4	0.07
Amazoncat-13k	logistic	aop*	93.0	77.4	61.7	85.7	47.1	23.50
Amazon-3M	tf-idf	aop	47.3	44.4	42.3	65.1	14.8	1,162.85